

*Supporting Information*

**High lithium and sodium anodic performance of nitrogen-rich ordered mesoporous carbon derived from alfalfa leaves by a ball-milling assisted template method**

Yongzhi Zhang, Yan Meng, Li Chen, Yong Guo \* and Dan Xiao\*

**Table S1.** ICP-AES results of the filtrate after reflux

<b>Element</b>	<b>Ca</b>	<b>K</b>	<b>Mg</b>	<b>Na</b>	<b>Fe</b>	<b>Al</b>	<b>Mn</b>	<b>Sr</b>	<b>Ni</b>	<b>Ba</b>	<b>Zn</b>
<b>t</b>	<b>17.9</b>	<b>11.8</b>									
<b>wt‰</b>	<b>4</b>	<b>7</b>	<b>4.34</b>	<b>1.33</b>	<b>0.92</b>	<b>0.64</b>	<b>0.21</b>	<b>0.09</b>	<b>0.04</b>	<b>0.03</b>	<b>0.03</b>

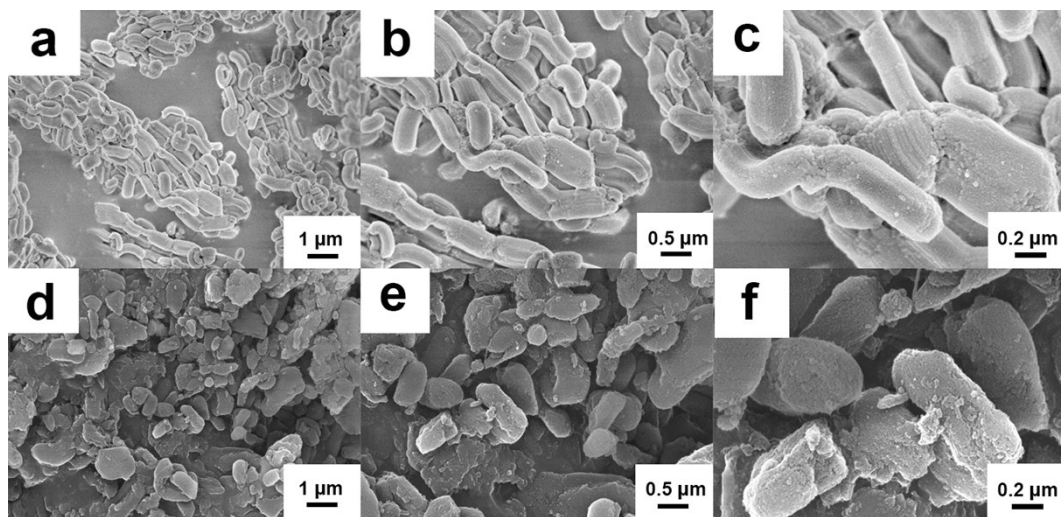


**Fig. S1** SEM images in different magnifications of SBA-15 template (a, b and c) and the re-ALs/SBA-15 composite (d, e and f).

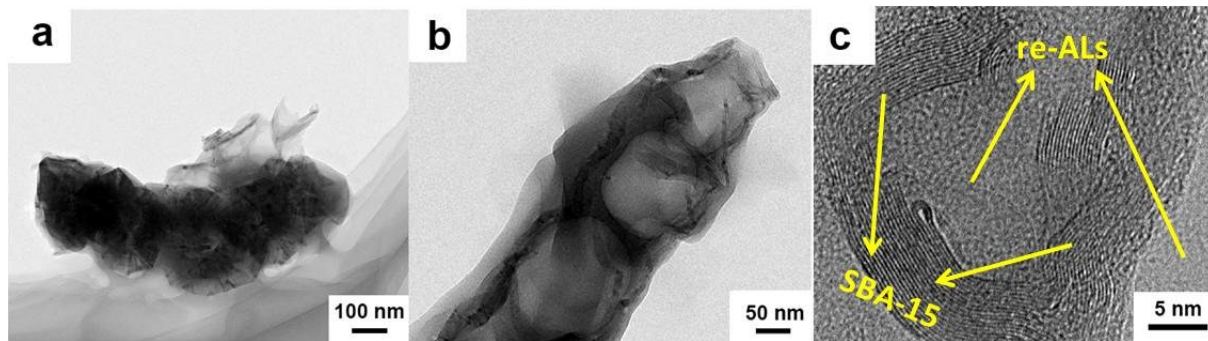


**Fig. S2** TEM (a and b) and HR-TEM (c) of the re-ALs/SBA-15 composite.

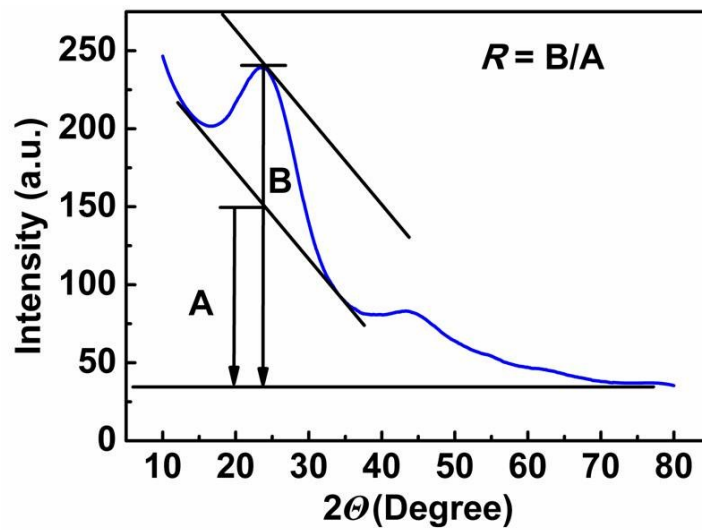


**Fig. S3** Scheme illustrating the R values calculation based on XRD patterns for ALNOMC.

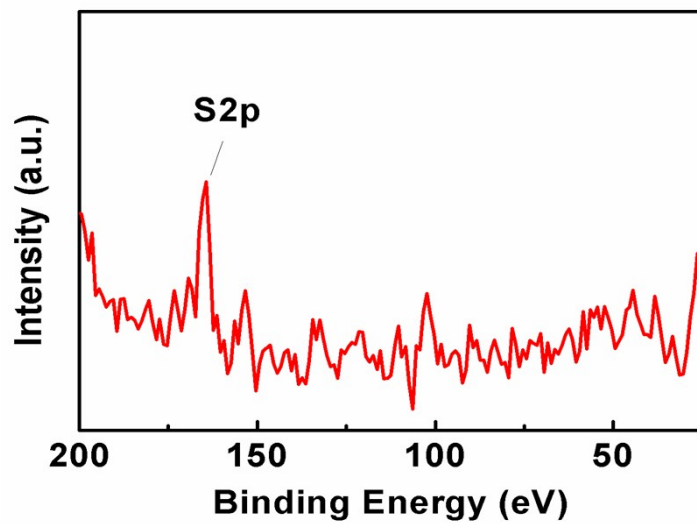


**Fig. S4** The partial XPS spectrum of ALNOMC.

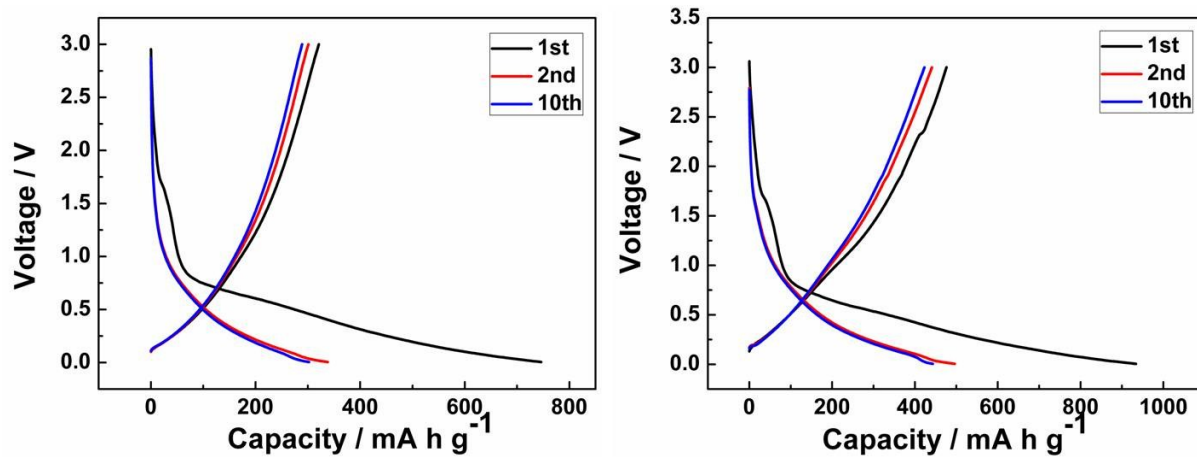


**Fig. S5** Charge-discharge curves of ALC (a) and re-ALC (b) at  $0.1 \text{ A g}^{-1}$ .

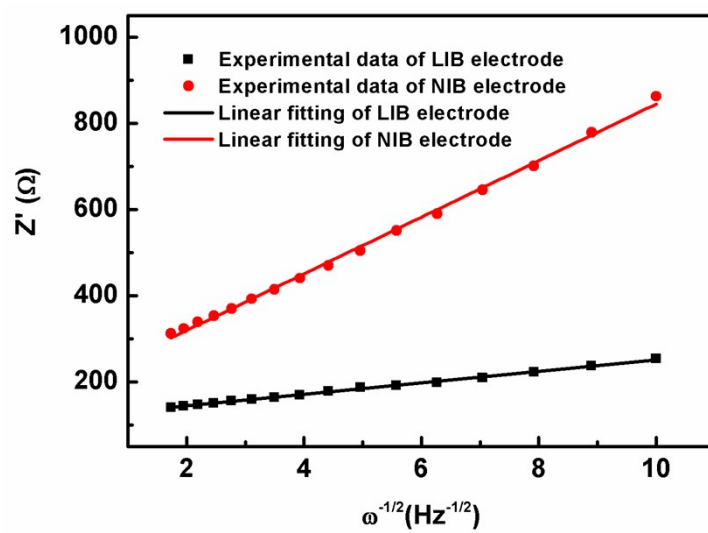


**Fig. S6** The relationship between  $Z'$  and reciprocal square root of frequency ( $\omega^{-1/2}$ ) for LIB and NIB electrodes of ALNOMC.

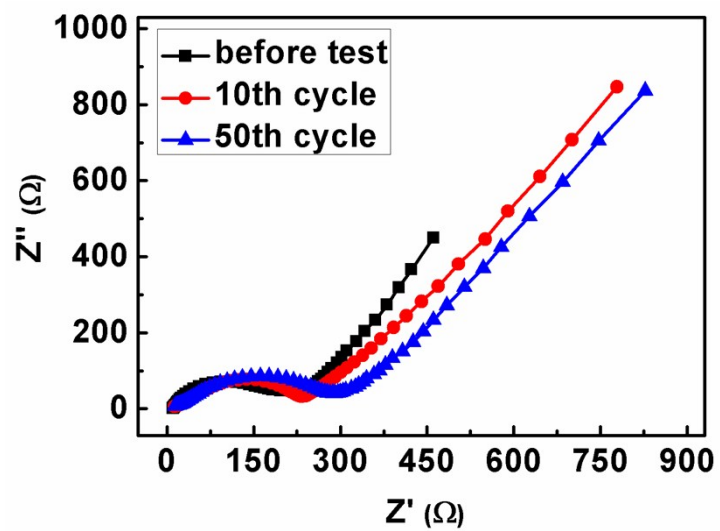


**Fig. S7** Electrochemical impedance spectra of ALNOMC electrodes before and after 10 and 50 cycles for NIBs.